ROBUST ALGORITHM FOR ACTIVE FEEDBACK CONTROL OF NARROWBAND NOISE

Maciej Niedźwiecki, Michał Meller and Maciej Gajdzica

Faculty of Electronics, Telecommunications and Computer Science, Department of Automatic Control
Gdańsk University of Technology, ul. Narutowicza 11/12, Gdańsk, Poland
maciekn@eti.pg.gda.pl, michal.meller@eti.pg.gda.pl

ABSTRACT

The problem of active control of narrowband acoustic noise is considered. It is shown that the proposed earlier feedback control algorithm called SONIC (self-optimizing narrowband interference canceller), based on minimization of the L_2-norm performance measure, can be re-derived using the L_1 approach. The resulting robust SONIC algorithm is more robust to heavy-tailed measurement noise, such as the α-stable noise, than the original SONIC.

Index Terms— active noise control, adaptive filtering

1. INTRODUCTION

Active control of acoustic noise is a long-standing problem, which has been studied for more than 30 years [1]–[4] and found its way to many challenging applications, such as attenuation of low-frequency noise in heating, ventilation and air-conditioning (HVAC) systems [5]–[6], active headsets [7]–[8] and systems that provide quiet zones in cars, trains, planes etc. [9]–[13] – see [14] for more examples of successful application of this technique.

Active noise control (ANC) is achieved by means of generating an "antinoise" – when two acoustic waves with the same amplitude but opposite polarity meet at a certain point in space, the sound is locally cancelled due to phenomenon known as destructive interference. ANC systems usually operate in the low frequency range (typically up to 500 Hz), i.e., in the range where passive approach to unwanted sound attenuation (sound absorbers, acoustic barriers) is hardly applicable for technical and/or economic reasons.

ANC systems are usually divided into feedforward schemes, which in addition to the error signal (measured at the system output), incorporate the so-called reference signal (measured by the sensor placed close to the source of unwanted sound), and feedback schemes that rely exclusively on the error signal.

Feedforward systems, which are capable of suppressing both narrowband and broadband noise, are usually controlled by the filtered-x least mean squares (FxLMS) algorithms or their modifications [1]–[4].

In the case of feedback systems, which can deal only with the narrowband noise, the most popular solutions are those based on the internal model principle [15], [16], phase-locked loop control [17], [18] and self-tuning regulation [19]–[21].

In this paper we will focus on the self-optimizing narrowband interference cancelling (SONIC) algorithm proposed in [19], capable of reducing nonstationary harmonic noise under plant (secondary path) uncertainties. We will show that SONIC, which was originally based on minimization of the quadratic performance measure, can be re-derived using the L_1-norm approach. The resulting algorithm is more robust to heavy-tailed measurement noise than the original algorithm.

2. PROBLEM STATEMENT

Denote by $t = \ldots, -1, 0, 1, \ldots$ the normalized (dimensionless) discrete time, and by q^{-1} the backward shift operator $q^{-1}x(t) = x(t-1)$. We will consider the problem of reduction of a nonstationary complex-valued narrowband interference $d(t)$, observed at the output of a linear stable plant with unknown or partially unknown transfer function $K_p(q^{-1})$. In acoustical applications such a plant is usually referred to as a secondary path. We will assume that the open-loop system description has the form (see Fig. 1)

$$y(t) = K_p(q^{-1})u(t-1) + d(t) + v(t) \tag{1}$$

where $y(t)$ denotes the complex-valued system output, $u(t)$ denotes the input (control) signal and $v(t)$ is a wideband measurement noise – zero-mean circular white sequence with variance σ_v^2. Furthermore, we will assume that the interference signal $d(t)$ obeys the following narrowband random-walk model

$$d(t) = e^{j\omega_0}d(t-1) + e(t) \tag{2}$$

where $\omega_0 \in [0, \pi)$ is a known angular frequency and $e(t)$ denotes circular white noise, independent of $v(t)$, with variance σ_e^2.

The only assumption that will be made about the unknown plant is that it has nonzero gain at the frequency ω_0: $k_{\rm p} = K_p(e^{-j\omega_0}) \neq 0$.

This work was partially supported by the National Science Centre under the agreement DEC-2011/03/B/ST7/01882.

978-0-9928626-3-3/15/$31.00 ©2015 IEEE

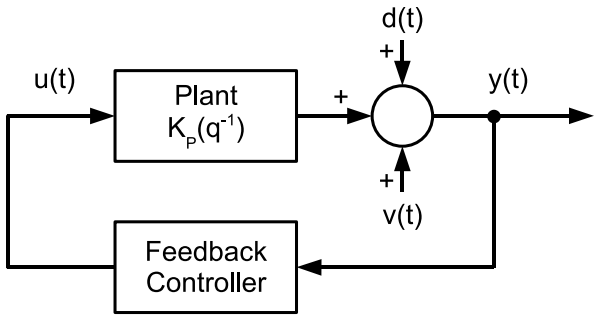

Fig. 1: Block diagram of the noise cancellation system

3. SONIC CONTROLLER

Derivation of the SONIC controller, presented in [19], was based on the steady-state system approximation. In order to cancel a narrowband signal $d(t)$, one should generate another narrowband signal $u(t)$, with the same frequency, which, after passing through the secondary path, will have the same amplitude as $d(t)$ but opposite polarity. Since linear systems operated in the steady state basically scale and time-shift sinusoidal inputs, it approximately holds that $K_p(q^{-1})u(t) \cong k_p u(t)$. Applying this approximation to (1), one obtains

$$y(t+1) \cong k_p u(t) + d(t+1) + v(t+1) \tag{3}$$

which leads to the following "idealized" cancelling rule

$$u(t) = -\frac{d(t+1)}{k_p}$$

based on the assumption that the disturbance signal is known ahead of time. A more realistic control rule has the form

$$\begin{aligned} \widehat{d}(t+1|t) &= e^{j\omega_0}[\widehat{d}(t|t-1) + \mu_0 y(t)] \\ u(t) &= -\frac{\widehat{d}(t+1|t)}{k_p} \end{aligned} \tag{4}$$

where $\widehat{d}(t+1|t)$ denotes the predicted value of $d(t+1)$ and $\mu_0 > 0$ is a small real-valued adaptation gain. Under such a control the cancelling error $c(t) = d(t) - \widehat{d}(t|t-1)$ can be expressed in the form

$$c(t+1) = e^{j\omega_0}(1-\mu_0)c(t) + e(t+1) - \mu_0 v(t) \tag{5}$$

which allows one to search for the optimal value of μ_0, e.g. the value that minimizes the variance of $c(t)$.

Interestingly, it can be shown that if the the true plant gain k_p is replaced in (4) by a nominal gain k_n, different from k_p ($\beta = k_p/k_n \neq 1$), and at the same time the real-valued adaptation gain μ_0 is replaced by the complex-valued gain $\mu = \mu_0/\beta$, the resulting control algorithm

$$\begin{aligned} \widehat{d}(t+1|t) &= e^{j\omega_0}[\widehat{d}(t|t-1) + \mu y(t)] \\ u(t) &= -\frac{\widehat{d}(t+1|t)}{k_n} \end{aligned} \tag{6}$$

performs identically as (4). This can be seen by analyzing the cancelling error $c(t) = d(t) - \beta\widehat{d}(t|t-1)$, which in the case of using (6) has the form

$$c(t+1) = e^{j\omega_0}(1-\beta\mu)c(t) + e(t+1) - \beta\mu v(t). \tag{7}$$

Quite clearly, after setting $\mu = \mu_0/\beta$, the error equation (7) becomes identical with (5), which means that, in spite of adopting the incorrect value of the plant gain, the system governed by (6) will achieve the same cancelling performance as the system governed by (4).

Since in practice the value of β is not known, one can adaptively search for such a value of μ which will not only compensate the modeling error, but will also optimize the closed-loop system performance. The solution proposed in [19] is based on minimization of the local measure of fit, made up of exponentially weighted "squares" of system outputs

$$V(t,\mu) = \sum_{\tau=1}^{t} \rho^{t-\tau} |y(\tau,\mu)|^2 \tag{8}$$

where ρ, $0 < \rho < 1$, denotes the forgetting constant which determines the effective averaging range. The recursive Newton-Raphson type algorithm for minimization of (8) has the form

$$\widehat{\mu}(t) = \widehat{\mu}(t-1) - \left[\frac{\partial^2 V(t,\widehat{\mu}(t-1))}{\partial\mu\partial\mu^*}\right]^{-1} \frac{\partial V(t,\widehat{\mu}(t-1))}{\partial\mu^*} \tag{9}$$

where

$$\frac{\partial}{\partial\mu} = \left[\frac{\partial}{\partial\mu_R} - j\frac{\partial}{\partial\mu_I}\right], \quad \frac{\partial}{\partial\mu^*} = \left[\frac{\partial}{\partial\mu_R} + j\frac{\partial}{\partial\mu_I}\right]$$
$$\mu_R = \mathrm{Re}[\mu], \quad \mu_I = \mathrm{Im}[\mu]$$

denote operations of symbolic differentiation with respect to a complex variable, used in the so-called Wirtinger calculus, applicable to nonanalytic functions, such as (8) – for details see [22].

For the quadratic cost function (8), one arrives at the following control algorithm, further referred to as SONIC (self-optimizing narrowband interference canceller) [19]

$$\begin{aligned} z(t) &= e^{j\omega_o}\left[(1-c_\mu)z(t-1) - c_\mu \frac{y(t-1)}{\widehat{\mu}(t-1)}\right] \\ r(t) &= \rho r(t-1) + |z(t)|^2 \\ \widehat{\mu}(t) &= \widehat{\mu}(t-1) - \frac{z^*(t)y(t)}{r(t)} \\ \widehat{d}(t+1|t) &= e^{j\omega_o}[\widehat{d}(t|t-1) + \widehat{\mu}(t)y(t)] \\ u(t) &= -\frac{\widehat{d}(t+1|t)}{k_n} \end{aligned} \tag{10}$$

where $z(t) = \partial y(t, \widehat{\mu}(t-1))/\partial \mu$, $r(t) = \partial^2[V(t, \widehat{\mu}(t-1))] /\partial \mu \partial \mu^*$, and $c_\mu > 0$ denotes a small user-dependent constant. We note that derivation of the sensitivity derivative $z(t)$ in a way that allows one to avoid its dependence on the unknown modeling error β is rather tricky - for more details see [19].

4. ROBUST SONIC

It is known that controllers based on minimization of L_1-type performance measures are more robust than their L_2 counterparts, e.g. they are more resistant to impulsive noise. Following this general observation, we will replace the quadratic cost function (8) with

$$V(t,\mu) = \sum_{\tau=1}^{t} \rho^{t-\tau} |y(\tau,\mu)|. \tag{11}$$

The algorithm that minimizes (11) will be further referred to as robust SONIC. Similarly as before, the complex-valued gain μ will be updated using the Newton-Raphson algorithm (9). However, since the cost function (11) is convex but non-differentiable at certain points, some derivatives will be replaced with their generalized versions called subderivatives.

Observe that

$$V(t,\mu) = \rho V(t-1,\mu) + |y(t,\mu)|$$

and hence

$$\begin{aligned} \frac{\partial V(t,\mu)}{\partial \mu^*} &= \rho \frac{\partial V(t-1,\mu)}{\partial \mu^*} + \frac{\partial |y(t,\mu)|}{\partial \mu^*} \\ \frac{\partial^2 V(t,\mu)}{\partial \mu \partial \mu^*} &= \rho \frac{\partial^2 V(t-1,\mu)}{\partial \mu \partial \mu^*} + \frac{\partial^2 |y(t,\mu)|}{\partial \mu \partial \mu^*}\,. \end{aligned} \tag{12}$$

Let

$$g(y) = |y| = \sqrt{yy^*}$$

where, for clarity reasons, the dependence of y on μ was suppressed. Using the chain rule of Wirtinger calculus, one obtains

$$\frac{\partial g(\mu)}{\partial \mu^*} = \nabla_y g(y) \frac{\partial y}{\partial \mu^*} + \nabla_{y^*} g(y) \frac{\partial y^*}{\partial \mu^*} \tag{13}$$

where ∇_y and ∇_{y^*} denote subderivatives with respect to y and y^*, respectively. Combining (3) with (10), one arrives at

$$y(t) \cong d(t) - \beta \widehat{d}(t|t-1) + v(t)$$

and

$$\frac{\partial y(t)}{\partial \mu^*} = -\beta \frac{\partial \widehat{d}(t|t-1)}{\partial \mu^*}\,.$$

Since in Wirtinger calculus μ and μ^* are treated as independent variables, and $\widehat{d}(t|t-1)$ does not depend explicitly on μ^*, it holds that $\partial y/\partial \mu^* = 0$ and consequently the first term on the right hand side of (13) is zero. To evaluate the second term, note that

$$\nabla_{y^*} g(y) = \frac{y}{2\sqrt{yy^*}}$$

which leads to

$$\frac{\partial |y|}{\partial \mu^*} = f(y) \frac{\partial y^*}{\partial \mu^*}\,, \quad f(y) = \frac{y}{2|y|}\,. \tag{14}$$

When $y = 0$, the result of division by $|y|$ is defined (here and below) as 0.

In a similar way one can compute the second-order derivative

$$\frac{\partial^2 |y|}{\partial \mu \partial \mu^*} = \frac{\partial}{\partial \mu} \left\{ f(y) \left[\frac{\partial y}{\partial \mu}\right]^* \right\} = \frac{\partial f(y)}{\partial \mu} \left[\frac{\partial y}{\partial \mu}\right]^*\,. \tag{15}$$

Note that

$$\frac{\partial f(y)}{\partial \mu} = \frac{1}{2|y|} \frac{\partial y}{\partial \mu} + \frac{y}{2} \frac{\partial}{\partial \mu} \left[\frac{1}{|y|}\right] \tag{16}$$

and (since $\partial y^*/\partial \mu = 0$)

$$\frac{\partial}{\partial \mu} \left[\frac{1}{|y|}\right] = \nabla_y \left[\frac{1}{|y|}\right] \frac{\partial y}{\partial \mu} = -\frac{1}{2y|y|} \frac{\partial y}{\partial \mu}\,. \tag{17}$$

Combining (15), (16) and (17), one arrives at

$$\frac{\partial^2 |y|}{\partial \mu \partial \mu^*} = \frac{1}{4|y|} \left|\frac{\partial y}{\partial \mu}\right|^2\,. \tag{18}$$

Assuming that $\widehat{\mu}(t-1)$ minimizes $V(t-1,\mu)$, and that the second-order derivative $\partial^2 V(t-1,\mu)/\partial \mu \partial \mu^*$ varies slowly with μ, i.e.,

$$\begin{aligned} \frac{\partial V(t-1, \widehat{\mu}(t-1))}{\partial \mu^*} &= 0 \\ \frac{\partial^2 V(t-1, \widehat{\mu}(t-1))}{\partial \mu \partial \mu^*} &\cong \frac{\partial^2 V(t-1, \widehat{\mu}(t-2))}{\partial \mu \partial \mu^*} \end{aligned}$$

one arrives at

$$\begin{aligned} \frac{\partial V(t-1, \widehat{\mu}(t-1))}{\partial \mu^*} &= \frac{\partial |y(t, \widehat{\mu}(t-1))|}{\partial \mu^*} \\ \frac{\partial^2 V(t, \widehat{\mu}(t-1))}{\partial \mu \partial \mu^*} &\cong \rho \frac{\partial^2 V(t-1, \widehat{\mu}(t-2))}{\partial \mu \partial \mu^*} \\ &\quad + \frac{\partial^2 |y(t, \widehat{\mu}(t-1))|}{\partial \mu \partial \mu^*}\,. \end{aligned} \tag{19}$$

According to (9), (14), (15) and (19), the robust SONIC algorithm can be expressed in the form

$$\begin{aligned} z(t) &= e^{j\omega_o} \left[(1-c_\mu) z(t-1) - c_\mu \frac{y(t-1)}{\widehat{\mu}(t-1)}\right] \\ r(t) &= \rho r(t-1) + \frac{|z(t)|^2}{4|y(t)|} \\ \widehat{\mu}(t) &= \widehat{\mu}(t-1) - \frac{z^*(t) y(t)}{2r(t)|y(t)|} \\ \widehat{d}(t+1|t) &= e^{j\omega_o} [\widehat{d}(t|t-1) + \widehat{\mu}(t) y(t)] \\ u(t) &= -\frac{\widehat{d}(t+1|t)}{k_n}\,. \end{aligned} \tag{20}$$

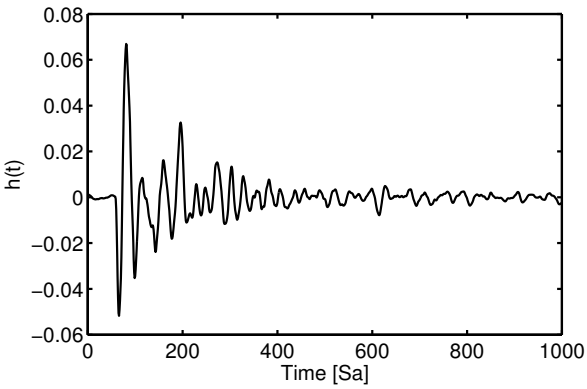

Fig. 2: Impulse response of the plant used in all simulations.

5. COMPUTER SIMULATIONS

A special simulation experiment was designed to compare behavior of the original SONIC controller and its robust version in the presence of heavy-tailed noise. The impulse response of the simulated plant, shown in Fig. 2, was obtained from a real-world identification experiment involving a 315 mm HVAC duct (8 kHz sampling was used).

The simulated disturbance signal was generated as follows: $d(t) = a(t)e^{j\omega_0 t}$, $a(t) = 1 + 0.005\cos(2\pi t/16000)$, where $\omega_0 = \pi/20$ (which corresponds to 200 Hz under 8 kHz sampling).

The nominal plant gain was set to $k_n = 1.6986 - 0.4843i$, while the true steady state gain of the simulated secondary path, measured at the frequency ω_0, was equal to $1.9036 + 0.4776i$. To guarantee fair comparison, the parameter ρ was adjusted so as to equalize performance of both algorithms in the presence of Gaussian distributed ($\sigma_v = 0.01$) measurement noise; to reduce the number of degrees of freedom, the parameter c_μ was in both cases set to the same value equal to 0.005. It was found that setting ρ to 0.9999 for the original algorithm, and to 0.9999285 for the robust one, resulted in only 0.5% difference in the corresponding mean squared steady state cancellation errors. When the same values of $\rho = 0.9999$ were used, the difference reached 11%.

To obtain statistically meaningful results, the cancellation efficiency was determined using combined time and ensemble averaging: 25 realizations of $v(t)$ were used, each covering 80000 samples, i.e., 5 periods of the modulating signal $a(t)$. Time averaging was started at the instant 50000, after the system has reached its steady state performance. The full adaptation mode was started at the instant 35000, after the quantities $r(t)$ in both algorithms stabilized their values. Finally, to avoid the risk of erratic system behavior, both algorithms were equipped with a "safety valve" – the upper allowable value of $|\widehat{\mu}(t)|$ was set to 0.01.

The performance of both algorithms in the presence of a heavy-tailed noise was checked using the symmetric α-stable (SαS) distributed $v(t)$.

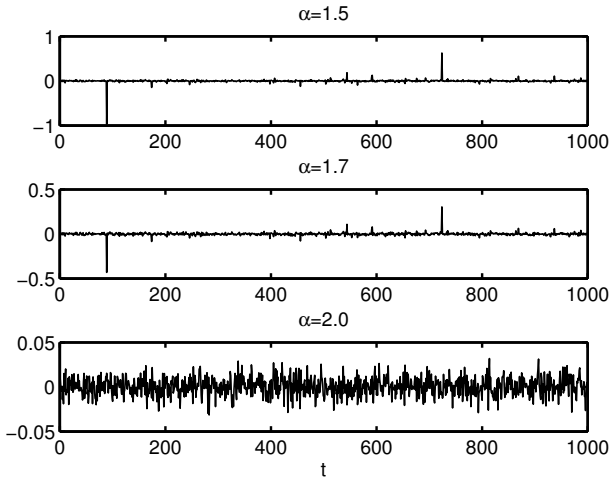

Fig. 3: Realizations α-stable random processes obtained for $\alpha \in \{1.5,\ 1.7,\ 2.0\}$, $\beta = 0$, $\gamma = 0$ and $\delta = 1$.

A probability distribution p is said to be stable if any linear combination of two independent, p-distributed random variables has the same distribution, up to the scale and location changes. Stable distributions are typically parametrized using 4 quantites: α, β, γ and δ. The quantities $\gamma \in (-\infty, \infty)$ and $\delta \in (0, \infty)$ are called location and scale parameters, respectively, and are "equivalents" of the mean and the variance of the distribution (note that, in general, these two moments do not exist for stable distributions). The other two parameters, $\alpha \in (0, 2]$ and $\beta \in [-1, 1]$, are called the stability parameter and the skewness parameter, respectively. Note that the case $\alpha = 2$ corresponds to Gaussian distribution. Fig. 3 shows three realizations α-stable random processes obtained for $\beta = 0$, $\gamma = 0$, $\delta = 1$ and three different values of α.

To prevent from excessive growth of the noise levels for smaller values of α, a special normalization procedure was employed. First, a non-normalized realization $r_u(t)$ of a SαS process was generated using $\gamma = 0$, $\delta = 1$, $\beta = 0$ and the desired value of α. Second, a sample median m of $|r_u(t)|$ was computed. Third, the normalized signal was obtained using

$$r_n(t) = \frac{0.01}{1.48m}\, r_u(t)\ .$$

In the Gaussian case the above procedure sets the standard deviation of $r_n(t)$ to 0.01. To obtain both the real and the imaginary part of a complex-valued measurement noise $v(t)$, generation of the normalized signal was performed twice. The same starting value of the random number generator was used for different values of α.

Fig. 4 shows the mean-squared steady state cancellation errors yielded by the two compared algorithms for different values of α. As α gets smaller, i.e., as the measurement noise becomes more heavy-tailed, the modified algorithm performs increasingly better than the original one. This confirms its improved robustness.

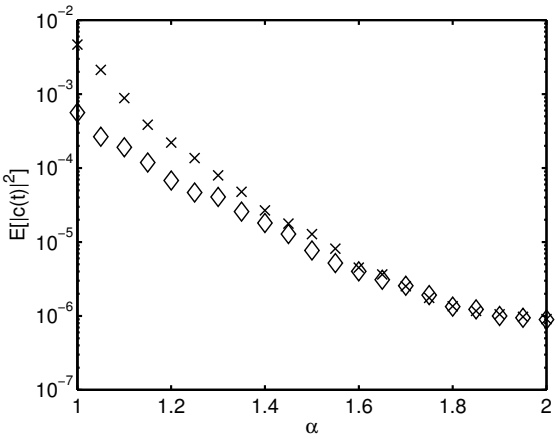

Fig. 4: Comparison of mean squared steady state cancellation errors yielded by the original SONIC algorithm (crosses) and robust SONIC (diamonds) for different values of α.

6. CONCLUSIONS

The problem of active feedback control of a nonstationary harmonic noise, in the presence of a heavy-tailed measurement noise, was considered. A new variant of the self-optimizing narrowband interference canceller (SONIC) was derived and checked using computer simulations. The new control algorithm, based on minimization of the L_1 performance measure, shows increased robustness compared with its previous, L_2-norm based version.

7. REFERENCES

[1] P. A. Nelson and S. J. Elliott, *Active control of sound*, Academic Press, 1992.

[2] S. M. Kuo and D. R. Morgan, *Active noise control systems*, Wiley, 1996.

[3] S. J. Elliott, *Signal processing for active noise control*, Academic Press, 2001.

[4] C. Hansen, S. Snyder, X. Qiu, L. Brooks, and D. Moreau, *Active Control of Noise and Vibration*, CRC Press, 2013.

[5] H.K. Pelton, S. Wise, and W.S. Sims, "Active HVAC noise control systems provide acoustical comfort", *Sound Vib.*, vol 28, pp. 14-18, 1994.

[6] S. Wise, J. F Nouvel, and V. Delemotte, "The first 1000 active duct silencers installed in HVAC systems – a summary of applications, successes and lessons learned," *Proc. InterNoise*, 6 p., 2000.

[7] A.J. Brammer, G.J. Pan, and R.B. Crabtree, "Adaptive feedforward active noise reduction headset for low-frequency noise," *Proc. of Active 97*, pp. 365-372, 1997.

[8] W. S. Gan and S. M. Kuo, "An Integrated Audio and Active Noise Control Headset," *IEEE Transactions on Consumer Electronics*, vol. 48, pp. 242-247, 2002

[9] T.J. Sutton, S.J. Elliot, A.M. McDonald, and T.J. Saunders, "Active control of road noise inside vehicles", *Noise Control Eng. J.*, vol. 42, pp. 137-147, 1994.

[10] S.M. Kuo and D. Vijayan, "Adaptive algorithms and experimental verification of feedback active noise control systems", *Noise Control Eng. J.*, vol. 42, pp. 37-46, 1994.

[11] C.R. Fuller and G.P. Gibbs, "Active control of interior noise in a business jet using piezoelectric actuators", *Proc. Noise-Con.*, pp. 389-394, 1994.

[12] H. Sano, "Modern advancements in passive and active noise and vibration control technology in automobiles,", *Proc. InterNoise*, 14 p., 2011.

[13] X. Zhang and X. Qiu, "Local active control of noise in a train compartment," *Proc. InterNoise*, 6 p., 2011.

[14] Y. Kajikawa, W.-S. Gan, and S. M. Kuo, "Rencent advances on active noise control: open issues and innovative applications," *APSIPA Trans. on Signal and Information Processing*, vol. 1, 2012.

[15] G. Feng and M. Palaniswami, "A stable adaptive implementation of the internal model principle," *IEEE Trans. Automat. Control*, vol. 37, pp. 1220–1225, Aug. 1992.

[16] I. Landau, A. Constantinescu, and D. Rey, "Adaptive narrow band disturbance rejection applied to an active suspension - an internal model principle approach," *Automatica*, vol. 41, pp. 563–574, Apr. 2005.

[17] M. Bodson and S. Douglas, "Adaptive algorithms for the rejection of sinusoidal disturbances with unknown frequency," *Automatica*, vol. 33, pp. 2213–2221, Dec. 1997.

[18] X. Guo and M. Bodson, "Adaptive rejection of multiple sinusoids of unknown frequency," in *Proc. European Control Conference*, pp. 121–128, 2007.

[19] M. Niedźwiecki and M. Meller, "A new approach to active noise and vibration control – Part I: the known frequency case", *IEEE Transactions on Signal Processing*, vol. 57, pp. 3373-3386, 2009.

[20] M. Niedźwiecki and M. Meller, "A new approach to active noise and vibration control – Part II: the unknown frequency case", *IEEE Transactions on Signal Processing*, vol. 57, pp. 3387-3398, 2009.

[21] M. Niedźwiecki and M. Meller, "Self-optimizing adaptive vibration controller", *IEEE Transactions on Automatic Control*, vol. 54, pp. 2087-2099, 2009.

[22] S. Haykin, *Adaptive Filter Theory*, Prentice-Hall, 1979.